

Electronic Supplementary Information

Redox-active diaminoazobenzene complexes of rhodium(III): synthesis, structure and spectroscopy

Sima Roy, Shuvam Pramanik, Tapas Ghorui, Soumitra Dinda, Sarat Chandra Patra and Kausikisankar

Pramanik*

Department of Chemistry, Inorganic Chemistry Section, Jadavpur University, Kolkata – 700032, India.

E-mail: kpramanik@hotmail.com; Tel: +91 94333 66013

Experimental Section

Physical Measurements

The elemental analyses (C, H, N) were performed with a Perkin- Elmer model 2400 series II elemental analyzer. FT-IR spectra were recorded on Perkin-Elmer L1600300 spectrometer. ¹H and ¹³C spectral measurement was carried out on Bruker 400 and 300 MHz spectrometers with TMS as an internal reference. ³¹P NMR spectra were obtained using a Bruker Avance 500 MHz spectrometer operating at 202.45 MHz. The electrospray ionization mass spectra (ESI-MS positive) were measured in acetonitrile HRMS spectrometers (Model: QTOF Micro YA263). Electrochemical measurements were carried out at 27°C with VersaStat II Princeton Applied Research potentiostat/galvanostat under argon atmosphere. The cell contained a Pt working electrode and a Pt wire auxiliary electrode. Tetrabutylammonium hexafluorophosphate (Bu_4NPF_6) was used as a supporting electrolyte and the potentials are referenced to the Ag/AgCl electrode without junction correction. The value of the Fc^+/Fc couple under similar experimental conditions is found to be 0.462 V vs Ag/AgCl .The electronic spectra in dichloromethane solution were obtained using a Perkin-Elmer LAMDA 25 spectrophotometer with a solute concentration of about 10^{-5} M. Electron paramagnetic resonance (EPR) spectra were recorded in standard quartz EPR tubes using JEOL JES-FA200 X-band spectrometer. The EPR spectra were simulated by Easy Spin software.¹

Crystallographic studies

X-ray intensity data for compound **2** and **3** were measured at 298(2) K on a Bruker AXS SMART APEX II equipped with a CCD diffractometer using a graphite monochromator ($Mo\text{ K}\alpha, \lambda = 0.71073\text{ \AA}$). Metal atoms were located by direct methods using the program SHELXS-97,² and the rest of the non-hydrogen atoms emerged from successive Fourier synthesis. The structures were refined by full-matrix least squares procedures on F^2 .³ All non-hydrogen atoms were refined anisotropically. The refinement and all further calculations were carried out using SHELXL-97.⁴ All the H atoms were included in calculated positions and treated as riding atoms using SHELXL default parameters, $U_{iso}(\text{H}) = 1.2U_{eq}(\text{C})$ except H1B, H4B, H5B, H8B atoms in **3**, which were located by Fourier difference synthesis and isotropically refined. Calculations were performed using the SHELXTL v 6.14 program package.⁵ Empirical absorption correction was applied using SADABS.⁶ Thermal ellipsoids are drawn at the 50% probability level. Molecular structure plots were drawn using the Oak Ridge thermal ellipsoid plot ORTEP.⁷

Computational details

Complexes **2** and **3** are diamagnetic at room temperature indicating their singlet ground state. The geometry optimization of these complexes was performed using their crystallographic coordinates in gas

phase in their singlet spin state without any ligand simplification by DFT method using the (R)B3LYP⁸ hybrid functional approach incorporated in GAUSSIAN 09 program package⁹. The optimized structural parameters are in general good agreement with the experimental values and the slight discrepancy arises due to the distortion in the crystal lattice that exists in real molecules. The nature of all the stationary points was checked by computing vibration frequencies, and all the species were found to be true potential energy minima, as no imaginary frequency were obtained (NImag = 0). On the basis of the optimized geometries, the absorption spectra in dichloromethane (CH_2Cl_2) media were calculated by the time-dependent density functional theory (TD-DFT)¹⁰ approach associated with the conductor-like polarizable continuum model (CPCM).¹¹ We computed the lowest 100 singlet–singlet transitions in absorption processes. We computed the lowest 100 singlet–singlet transitions and 100 singlet–triplet transitions in absorption processes and the results of the TD calculations were qualitatively similar to the observed spectra. To analyze the nature of absorption processes, natural transition orbital (NTO) analysis were performed.¹² This method offers the most compact representation of the transition density between the ground and excited states in terms of an expansion into single-particle transitions (hole and electron states for each given excitation). Here we refer to the unoccupied and occupied NTOs as “electron” and “hole” transition orbitals. The computed vertical transitions were calculated at the equilibrium geometry of the S_0 state and described in terms of one-electron excitations of molecular orbitals of the corresponding S_0 geometry. The calculated transitions with moderate intensities ($f \geq 0.02$) can be envisaged going from the lower to the higher energy region of the spectrum. The rhodium atom was described by a double- ζ basis set with the effective core potential of Hay and Wadt (LANL2DZ)¹³ and the 6-31+G* basis set¹⁴ was used for the other elements present in the complexes except P and Cl to optimize the ground state geometries. The 6-31G(d,p) basis set was used for P and Cl to optimize the compounds while hydrogen atom was optimized using 6-31G basis set. The calculated electronic density plots for frontier molecular orbitals were prepared by using the GaussView 5.0 software. GaussSum program, version 2.2¹⁵ was used to calculate the molecular orbital contributions from groups or atoms.

References

- [1] S. Stoll and A. Schweiger, EasySpin, a comprehensive software package for spectral simulation and analysis in EPR. *J. Magn. Reson.* 2006, **178**, 42–55.
- [2] G. M. Sheldrick; *SHELXS-97, Program for Crystal Structure Solution*; University of Göttingen: Göttingen, Germany, 1997.
- [3] G. M. Sheldrick, *Acta Crystallogr.*, 2008, **A64**, 112.
- [4] G. M. Sheldrick, *SHELXL-97, Program for Refining X-ray Crystal Structures*; University of Göttingen: Göttingen, Germany, 1997.

- [5] G. M. Sheldrick, *SHELXTL v. 6.14*, Bruker AXS Inc., Madison, WI, 2003.
- [6] G. M. Sheldrick, SADABS; Bruker AXS, Inc.: Madison, WI, 2007.
- [7] C. K. Johnson, *ORTEP*; Report ORNL-5138; Oak Ridge National Laboratory: Oak Ridge, TN, 1976.
- [8] (a) A. D. Becke, *J. Chem. Phys.*, 1993, **98**, 5648–5652; (b) C. Lee, W. Yang and R. G. Parr, *Phys. Rev. B*, 1988, **37**, 785–789.
- [9] M. J. Frisch, G. W. Trucks, H. B. Schlegel, G. E. Scuseria, M. A. Robb, J. R. Cheeseman, G. Scalmani, V. Barone, B. Mennucci, G. A. Petersson, H. Nakatsuji, M. Caricato, X. Li, H. P. Hratchian, A. F. Izmaylov, J. Bloino, G. Zheng, J. L. Sonnenberg, M. Hada, M. Ehara, K. Toyota, R. Fukuda, J. Hasegawa, M. Ishida, T. Nakajima, Y. Honda, O. Kitao, H. Nakai, T. Vreven, J. A. Montgomery Jr, J. E. Peralta, F. Ogliaro, M. Bearpark, J. J. Heyd, E. Brothers, K. N. Kudin, V. N. Staroverov, R. Kobayashi, J. Normand, K. Raghavachari, A. Rendell, J. C. Burant, S. S. Iyengar, J. Tomasi, M. Cossi, N. Rega, J. M. Millam, M. Klene, J. E. Knox, J. B. Cross, V. Bakken, C. Adamo, J. Jaramillo, R. Gomperts, R. E. Stratmann, O. Yazyev, A. J. Austin, R. Cammi, C. Pomelli, J. W. Ochterski, R. L. Martin, K. Morokuma, V. G. Zakrzewski, G. A. Voth, P. Salvador, J. J. Dannenberg, S. Dapprich, A. D. Daniels, O. Farkas, J. B. Foresman, J. V. Ortiz, J. Cioslowski and D. J. Fox, *GAUSSIAN 09 (Revision A.02)*, Gaussian, Inc., Wallingford, CT, 2009.
- [10] (a) J. Autschbach, T. Ziegler, S. J. A. Gisbergen and E. J. Baerends, *J. Chem. Phys.*, 2002, **116**, 6930–6940; (b) K. L. Bak, P. Jørgensen, T. Helgaker, K. Ruud and H. J. A. Jenson, *J. Chem. Phys.*, 1993, **98**, 8873–8887; (c) T. Helgaker and P. Jørgensen, *J. Chem. Phys.*, 1991, **95**, 2595–2601; (d) E. K. U. Gross and W. Kohn, *Adv. Quantum Chem.*, 1990, **21**, 255–291.
- [11] (a) M. Cossi, N. Rega, G. Scalmani and V. Barone, *J. Comput. Chem.*, 2003, **24**, 669–681; (b) M. Cossi and V. Barone, *J. Chem. Phys.*, 2001, **115**, 4708–4717; (c) V. Barone and M. Cossi, *J. Phys. Chem. A*, 1998, **102**, 1995–2001.
- [12] R. L. Martin, *J. Chem. Phys.*, 2003, **118**, 4775–4777.
- [13] (a) P. J. Hay and W. R. Wadt, *J. Chem. Phys.*, 1985, **82**, 299–310; (b) P. J. Hay and W. R. Wadt, *J. Chem. Phys.*, 1985, **82**, 270–283.
- [14] (a) M. S. Gordon, J. S. Binkley, J. A. Pople, W. J. Pietro and W. J. Hehre, *J. Am. Chem. Soc.*, 1982, **104**, 2797–2803; (b) J. S. Binkley, J. A. Pople, and W. J. Hehre, *J. Am. Chem. Soc.*, 1980, **102**, 939–947.
- [15] N. M. O'Boyle, A. L. Tenderholt and K. M. Langner, *J. Comput. Chem.*, 2008, **29**, 839–845.

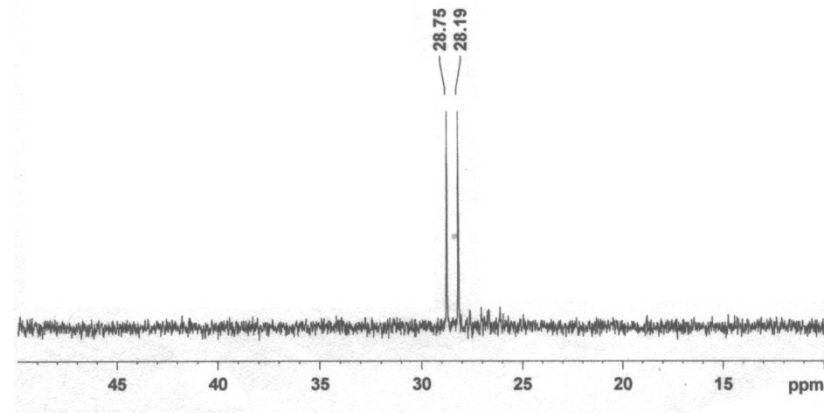
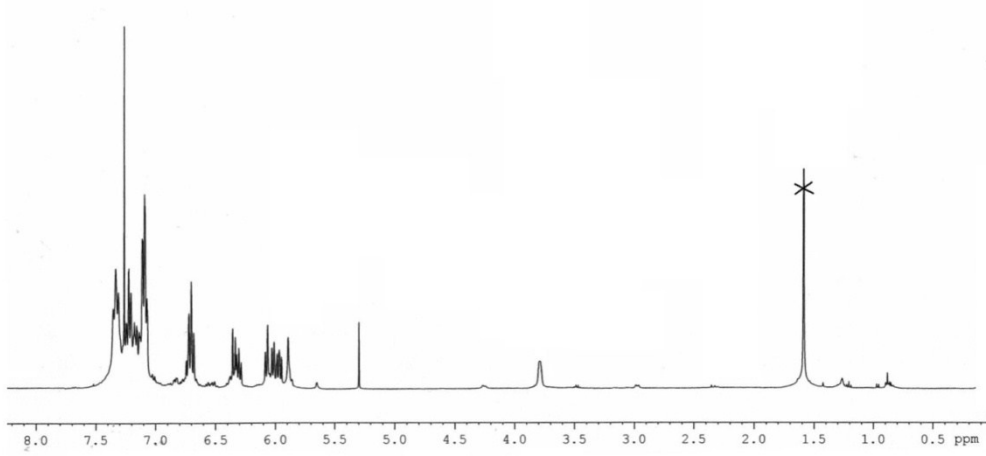
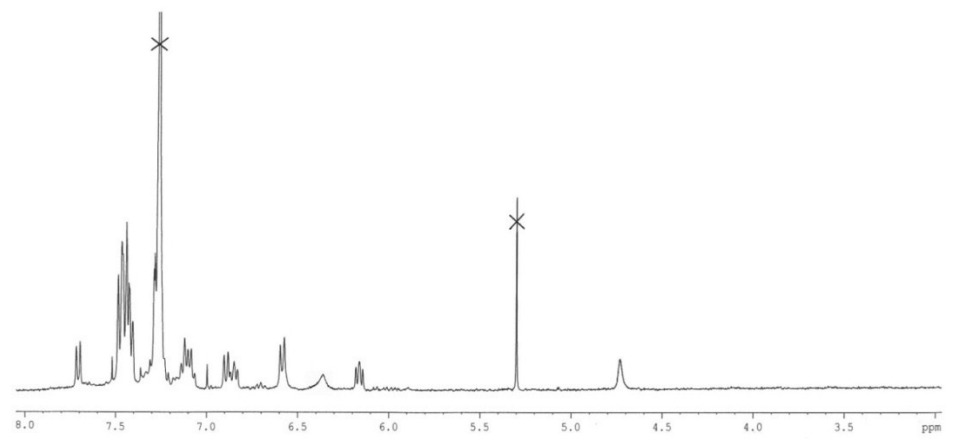


Fig. S1 ¹H NMR spectrum of **2** (top) and **3** (middle) and ³¹P NMR of **3** (bottom).

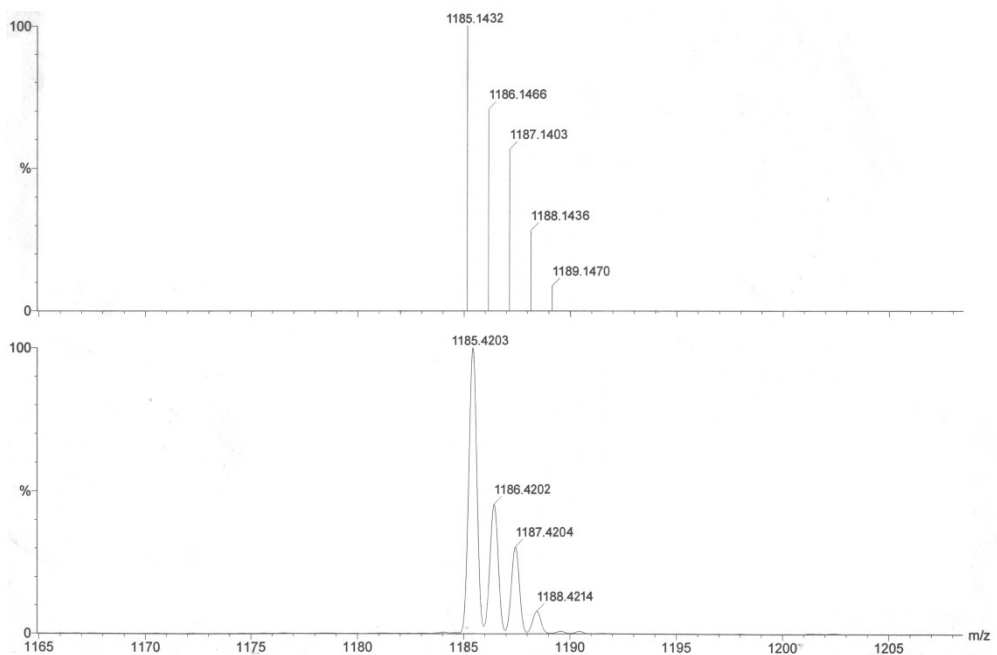
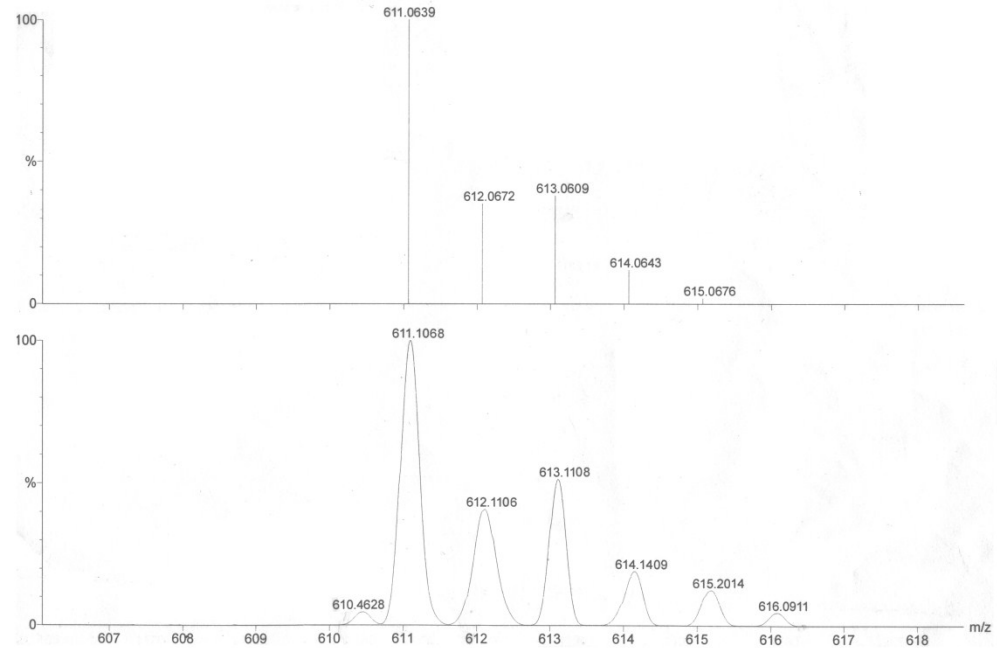


Fig. S2 High-resolution mass spectra of **2** (top) and **3** (bottom) compounds. (Expt.: below, Calcd.: above).

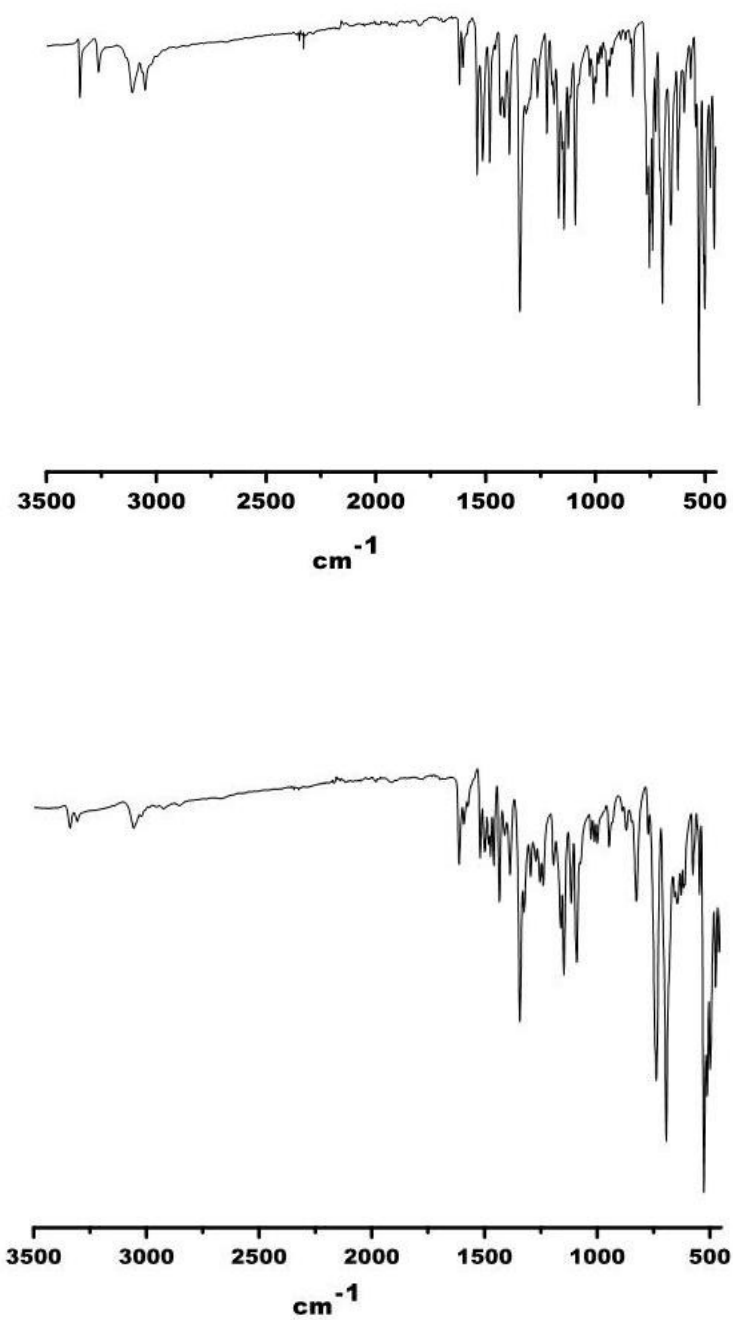


Fig. S3 FT-IR spectra of **2** (top) and **3** (bottom).

Table S1 Crystal data and structure refinement parameters for complex **2** and **3**

	[2]·2CH ₂ Cl ₂	[3]·3CH ₂ Cl ₂
Empirical formula	C ₃₂ H ₃₀ N ₄ PCl ₆ Rh	C ₆₃ H ₅₆ N ₈ P ₂ Cl ₈ Rh ₂
fw	817.18	1476.52
T/K	298(2)	298(2)
Cryst system	Triclinic	Monoclinic
Space group	<i>P</i> 	<i>P</i> 2(1)/ <i>n</i>
<i>a</i> /Å	10.8829(9)	19.6187(9)
<i>b</i> /Å	12.4756(10)	12.5476(6)
<i>c</i> /Å	14.0207(12)	25.9749(12)
α /deg	70.126 (5)	90
β /deg	89.504 (5)	93.411(2)
γ /deg	78.191 (5)	90
<i>V</i> /Å ³	1748.5(3)	6382.9(5)
<i>Z</i>	2	4
<i>D</i> _c /mg m ⁻³	1.552	1.536
μ /mm ⁻¹	1.022	0.949
<i>F</i> (000)	824	2984
cryst size/mm ³	0.36×0.22×0.15	0.41×0.28×0.17
θ /deg	1.78–27.52	1.57–30.33
measured reflns	28848	69802
unique reflns/ <i>R</i> _{int}	7857/ 0.0782	18894 /0.0578
GOF on <i>F</i> ²	1.016	1.076
R1, ^a wR2 ^b	0.0480, 0. 1221	0.0565, 0.1521
[<i>I</i> > 2σ(<i>I</i>)]		
R1, wR2 (all data)	0.0819, 0. 1376	0.0857, 0.1750

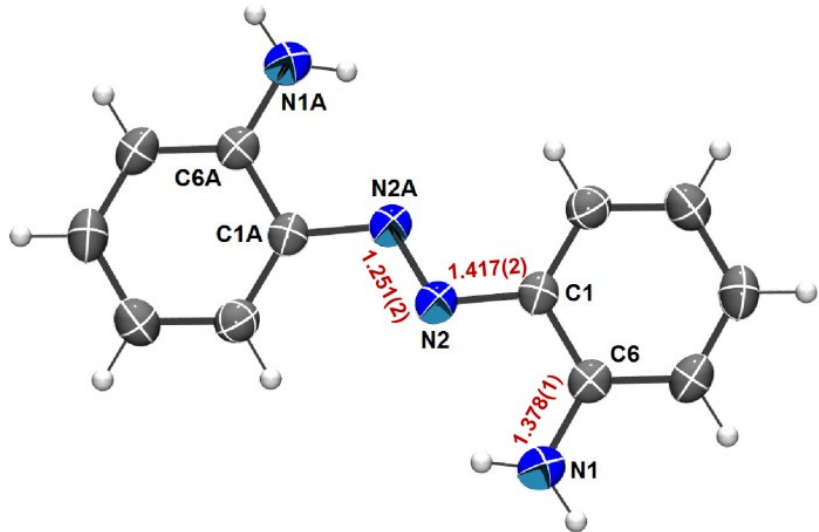


Fig. S4 ORTEP of ligand **1** at the 50% probability level,

Space group: *C2/c*, Crystal System: Monoclinic.

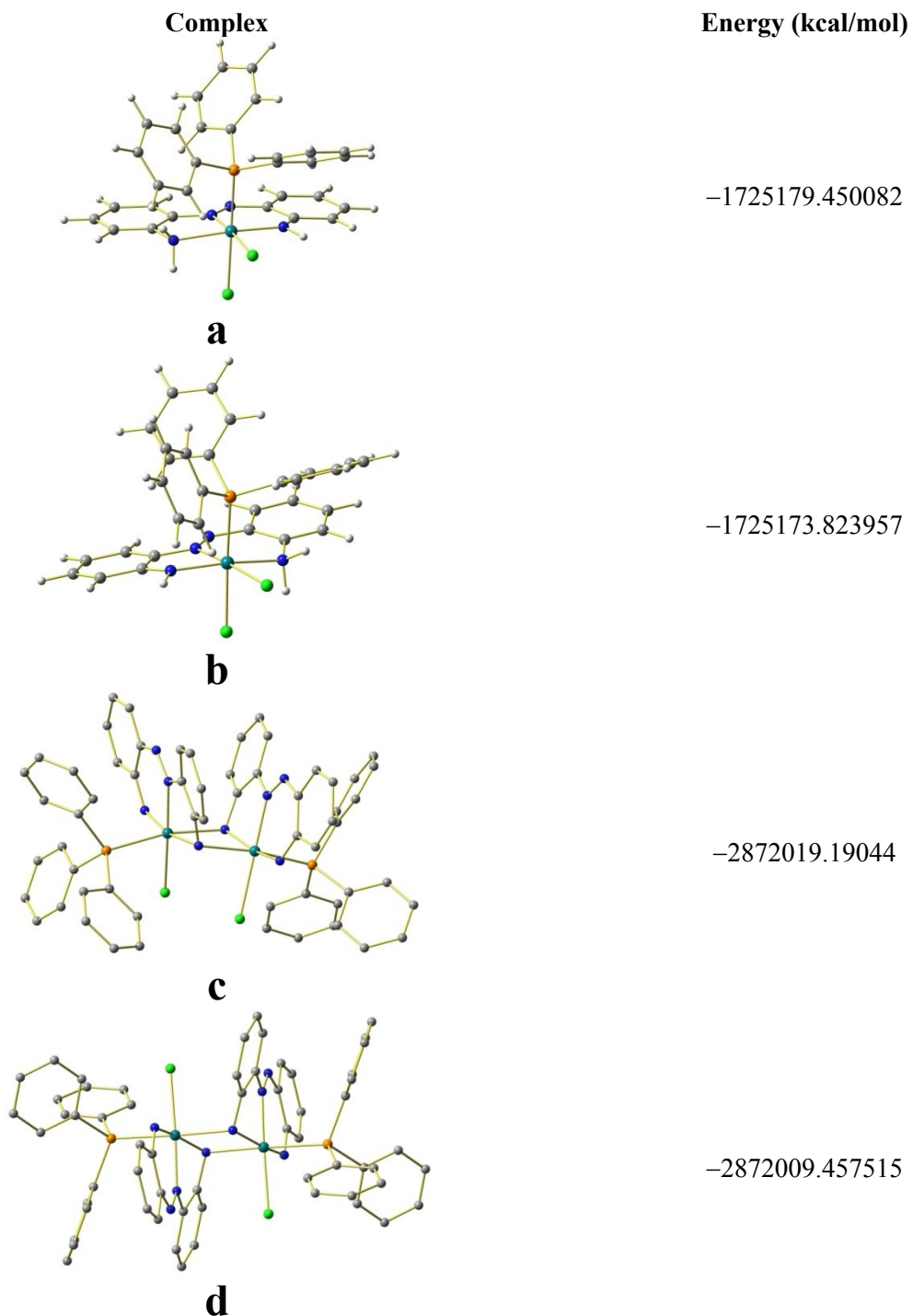


Fig. S5 Optimized molecular structures of **2** (coordination mode B)(a), **2'** (coordination mode C) (b), *syn*-**3** (c) and *anti*-**3** (d) (Rh: cyan, N: blue, C: grey, Cl: green, P: saffron. Hydrogen atoms are omitted for clarity). [$E_2 - E_{2'} = -5.63$ kcal/mol], [$E_{\text{syn-}3} - E_{\text{anti-}3} = -9.77$ kcal/mol].

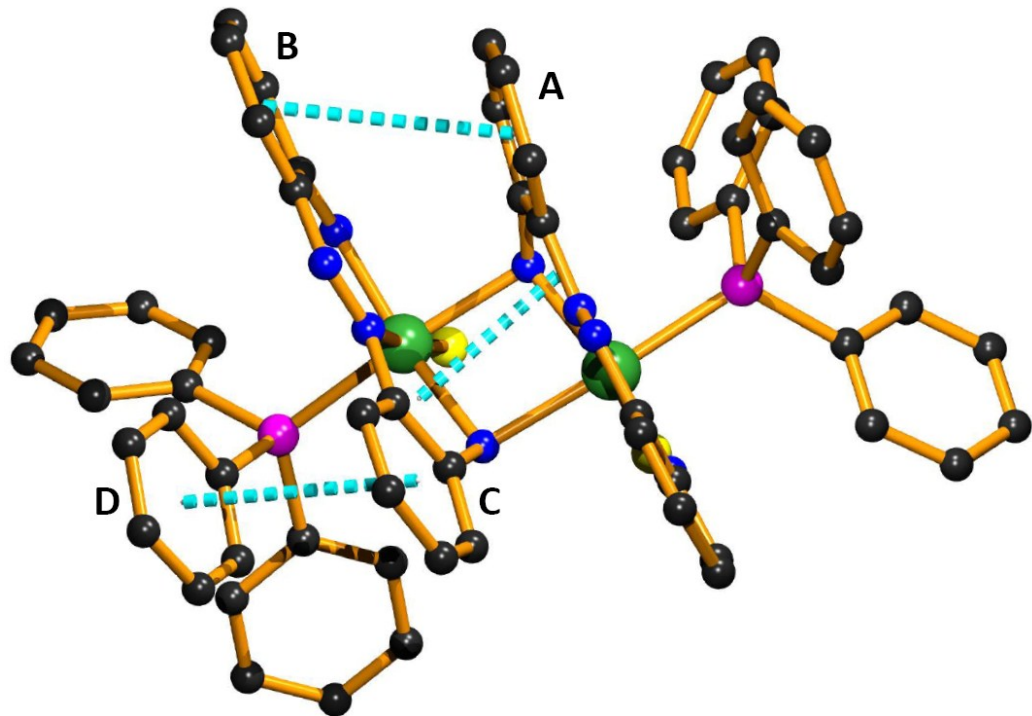
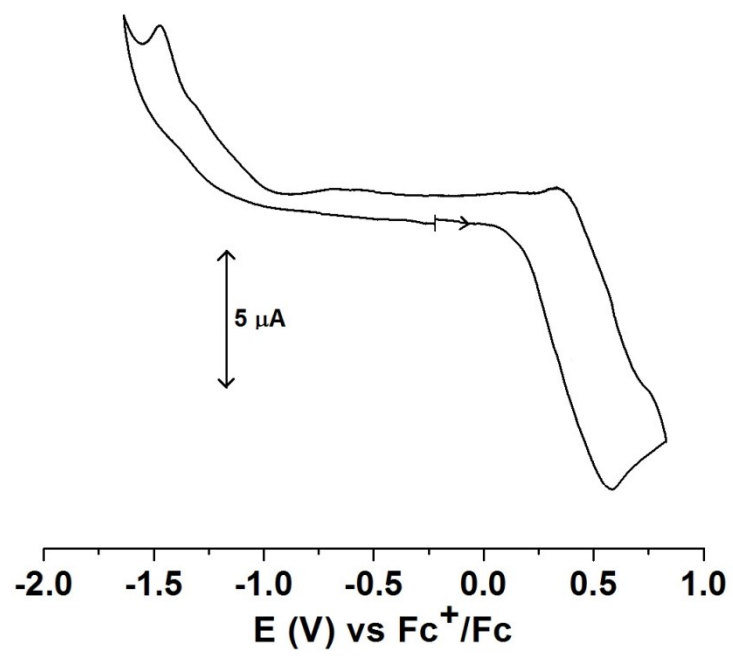


Fig. S6 Intramolecular noncovalent H-bonding and $\text{Ph}_\pi-\text{Ph}_\pi$ stacking interactions. (The relevant distances are tabulated in Table S2)

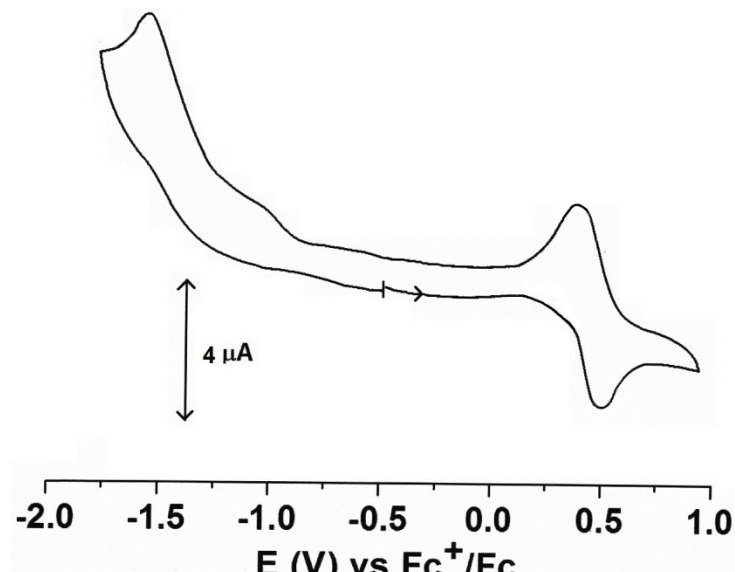
Table S2 Intramolecular $\pi-\pi$ stacking parameters^a for compound 3

Stacking params	Chelate-chelate	phenyl-phenyl	
		A-B	C-D
$d(c_i-c_j) \text{ \AA}/\alpha^\circ$	2.732(3)/24.4(2)	3.849(3)/13.4(2)	3.642(3)/12.4(2)
$d(\perp c_i-P_j) \text{ \AA}/\beta^\circ$		3.354(2)/29.39	3.349(2)/23.09
$d(\perp c_j-P_i) \text{ \AA}/\beta'^\circ$		3.294(2)/31.14	3.434(2)/19.39

^a c = ring centroid, α = dihedral angle between rings, β and β' (slip angle) = angle between the vector c_i-c_j and the normal to plane P_i or P_j from c_i and c_j respectively, $d(c_i-c_j)$ = centroid-centroid distance, $d(\perp c_i-P_j)$ = \perp distance from c_i of P_i on ring P_i .



(a)



(b)

Fig. S7 Voltammogram of **2** in CH_2Cl_2 at 100 mV s^{-1} scan rate (a) at 298 K (b) 210 K .

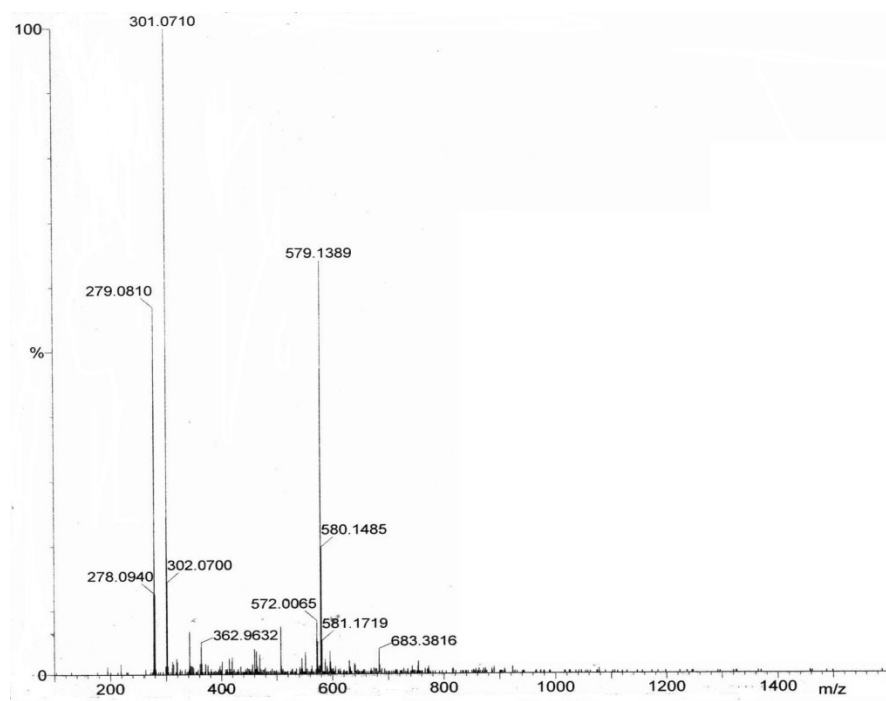
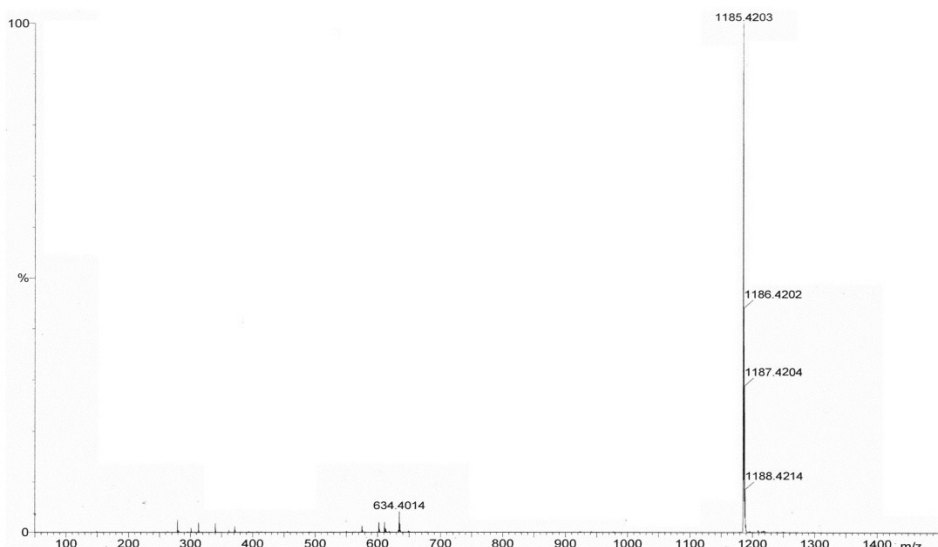


Fig. S8 High-resolution mass spectra of **3** (top) and its chemically oxidized species (bottom) in CH_3CN at room temperature.

Table S3 Selected optimized geometrical parameters of **2** and **3** in the ground and lower lying triplet excited states at B3LYP level

Bond Lengths (Å)					
2		3			
Rh1–N5	2.13170	Rh1–N7	2.02579	Rh2–N13	2.02766
Rh1–N10	1.99763	Rh1–N10	2.02698	Rh2–N16	2.02811
Rh1–N8	2.01214	Rh1–N11	2.12043	Rh2–N17	2.12495
Rh1–Cl3	2.43725	Rh1–N17	2.19931	Rh2–N11	2.20092
Rh1–Cl4	2.43915	Rh1–Cl3	2.46012	Rh2–Cl4	2.46810
Rh1–P2	2.42474	Rh1–P5	2.43066	Rh2–P6	2.42346
N8–N9	1.27849	N7–C19	1.32574	N13–C72	1.32484
C31–N5	1.45612	N11–C38	1.40461	N17–C91	1.40540
C12–N10	1.32028	N9–N10	1.27600	N15–N16	1.27656

Bond Angles (°)					
2		3			
P2–Rh1–Cl3	86.397	Cl3–Rh1–P5	86.286	Cl4–Rh2–P6	89.809
P2–Rh1–Cl4	176.635	Cl3–Rh1–N7	84.402	Cl4–Rh2–N11	82.958
P2–Rh1–N5	96.122	Cl3–Rh1–N10	174.188	Cl4–Rh2–N13	84.542
P2–Rh1–N8	97.662	Cl3–Rh1–N11	105.285	Cl4–Rh2–N16	173.851
P2–Rh1–N10	91.423	Cl3–Rh1–N17	83.691	Cl4–Rh2–N17	105.206
Cl3–Rh1–Cl4	90.479	P5–Rh1–N7	92.269	P6–Rh2–N11	170.726
Cl3–Rh1–N5	95.495	P5–Rh1–N10	95.057	P6–Rh2–N13	91.954
Cl3–Rh1–N8	175.585	P5–Rh1–N11	96.588	P6–Rh2–N16	93.074
Cl3–Rh1–N10	90.970	P5–Rh1–N17	168.469	P6–Rh2–N17	95.900
Cl4–Rh1–N5	82.923	N7–Rh1–N10	89.890	N11–Rh2–N13	93.123
Cl4–Rh1–N8	85.423	N7–Rh1–N11	167.230	N11–Rh2–N16	94.688
Cl4–Rh1–N10	89.877	N7–Rh1–N17	92.411	N11–Rh2–N17	80.501
N5–Rh1–N8	82.385	N10–Rh1–N11	80.205	N13–Rh2–N16	89.929
N5–Rh1–N10	170.346	N10–Rh1–N17	95.485	N13–Rh2–N17	167.451
N8–Rh1–N10	90.666	N11–Rh1–N17	80.637	N16–Rh2–N17	79.911

Table S4 Frontier Molecular Orbital Composition (%) in the Ground State for **2**

Orbital	MO	Energy (eV)	Contribution (%)						
			Rh	Azo	Amine	Amido	Ph	PPh ₃	Cl
156	L+5	-1.08	48	13	7	11	8	5	9
155	L+4	-1.19	3	0	1	0	12	82	1
154	L+3	-1.21	1	1	0	0	1	97	1
153	L+2	-1.42	1	1	1	0	0	98	0
152	L+1	-2.1	37	5	1	1	0	38	18
151	LUMO	-2.53	3	35	0	10	52	0	0
150	HOMO	-5.23	9	12	0	23	51	2	3
149	H-1	-6.21	3	0	0	0	5	2	90
148	H-2	-6.25	20	1	0	0	6	6	66
147	H-3	-6.37	15	0	0	0	5	3	78
146	H-4	-6.48	22	0	0	0	7	2	72
145	H-5	-6.71	2	10	1	2	71	4	11

HOMO–LUMO gap = 2.70 eV

Table S5 Frontier Molecular Orbital Composition (%) in the Ground State for **3**

Orbital	MO	Energy (eV)	Contribution (%)						
			Ligand						
			Rh	Azo	N _{amido(nb)}	N _{amido(b)}	Ph	Cl	PPh ₃
288	L+5	-0.99	0	0	0	1	5	1	91
287	L+4	-1.02	0	0	1	1	1	0	96
286	L+3	-1.64	8	8	1	7	13	5	30
285	L+2	-1.81	13	13	2	5	19	4	24
284	L+1	-2.18	31	31	6	-2	45	1	7
283	LUMO	-2.38	7	33	8	2	46	0	3
282	HOMO	-4.87	7	7	22	5	54	0	3
281	H-1	-5	11	11	24	1	54	1	0
280	H-2	-5.66	5	5	5	21	38	6	9
279	H-3	-5.87	6	6	1	12	55	6	13
278	H-4	-6.01	1	1	0	2	10	65	2
277	H-5	-6.32	0	0	0	0	11	60	6

HOMO-LUMO gap = 2.49 eV

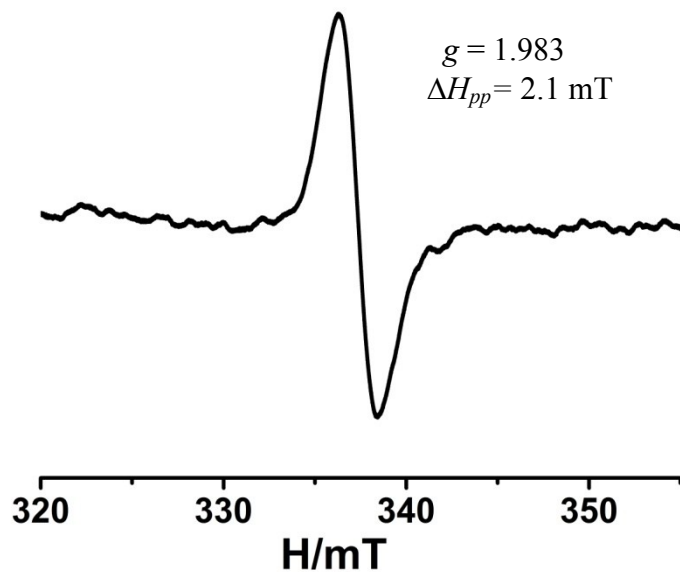


Fig. S9 X-band EPR spectrum of the oxidized species derived from **2** in CH_2Cl_2 with silver triflate at 77K. Instrument settings: microwave frequency, 9.419 GHz; power, 0.998 mW; modulation frequency, 100 kHz.

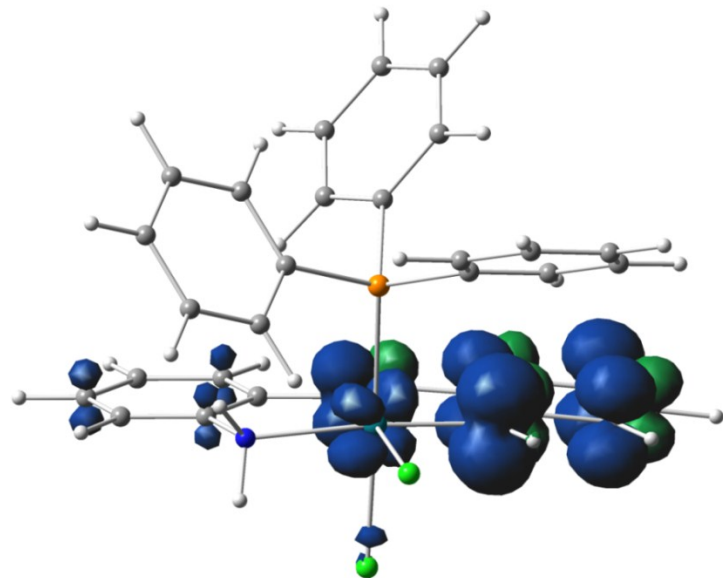


Fig. S10 Net spin density of $\mathbf{2}^{\bullet+}$ [$\rho_{\text{N(amido)}} = 46\%$, $\rho_{\text{Ph}} = 39\%$, $\rho_{\text{azo}} = 4\%$, $\rho_{\text{Rh}} = 9\%$].

Table S6 Main optical transition at the TD-DFT/B3LYP/6-311+G(d,p) + LANL2DZ Level for the complex **2** with composition in terms of molecular orbital contribution of the transition, Computed Vertical excitation energies, and oscillator strength in dichloromethane

Transition	CI	Composition	E(ev)	Oscillator strength (<i>f</i>)	λ_{heo}
$S_0 \rightarrow S_1$	0.67876	HOMO \rightarrow L+1 (92%)	2.0943	0.0130	592.01
$S_0 \rightarrow S_2$	0.69555	HOMO \rightarrow LUMO (97%)	2.2554	0.1643	549.73
$S_0 \rightarrow S_7$	0.46731 0.23533	H-1 \rightarrow LUMO (44%) H-5 \rightarrow L+1 (11%)	3.4375	0.0455	360.68
$S_0 \rightarrow S_8$	0.37616 0.23443	H-1 \rightarrow LUMO (28%) H-3 \rightarrow LUMO (11%)	3.4761	0.0642	356.67
$S_0 \rightarrow S_{10}$	0.38106 -0.33731 0.26696	HOMO \rightarrow L+3 (29%) H-4 \rightarrow LUMO (23%) H-2 \rightarrow LUMO (14%)	3.6134	0.0654	343.12
$S_0 \rightarrow S_{15}$	0.45606 -0.28294	H-6 \rightarrow LUMO (42%) H-5 \rightarrow LUMO (16%)	3.7994	0.1203	326.32
$S_0 \rightarrow S_{21}$	0.41084 -0.29398	H-5 \rightarrow L+1 (34%) H-2 \rightarrow L+1 (17%)	4.0538	0.2817	305.85
$S_0 \rightarrow S_{45}$	0.50524	HOMO \rightarrow L+11 (51%)	4.7420	0.1486	261.46

		Hole	Electron
648 nm	S_1 $w = 0.92$ 2.0943 (0.0130) 592.01 nm		
	$^1\text{LMCT}/^1\text{ILCT}/^1\text{LLCT}$ $\pi(\text{N}_{\text{amido}} + \text{Ph}) \rightarrow 4d_z^2(\text{Rh}) + \pi^*(\text{azo}) + 3p(\text{Cl})$		
606 nm	S_2 $w = 0.97$ 2.2554 (0.1643) 549.73 nm		
	$^1\text{ILCT}$ $\pi(\text{N}_{\text{amido}} + \text{Ph}) \rightarrow \pi^*(\text{azo} + \text{Ph})$		
365 nm	S_7 $w = 0.44$ 3.4375 (0.0455) 360.68 nm		
	$^1\text{ILCT}/^1\text{LLCT}$ $\pi(\text{Ph} + \text{azo}) + 3p(\text{Cl}) \rightarrow \pi^*(\text{azo} + \text{Ph})$		
273 nm	S_{45} $w = 0.51$ 4.7420 (0.1486) 261.46		
	$^1\text{ILCT}$ $\pi(\text{N}_{\text{amido}} + \text{Ph}) \rightarrow \pi^*(\text{Ph})$		

Fig. S11 Natural transition orbitals (NTOs) for complex **2** illustrating the nature of singlet excited states in the absorption bands in the range 250–700 nm. For each state, the respective number of the state, transition energy (eV), and the oscillator strength (in parentheses) are listed. Shown are only occupied (holes) and unoccupied (electrons) NTO pairs that contribute more than 40% to each excited state.

Table S7 Main optical transition at the TD-DFT/B3LYP/6-311+G(d,p) + LANL2DZ Level for the complex **3** with composition in terms of molecular orbital contribution of the transition, Computed Vertical excitation energies, and oscillator strength in dichloromethane

Transition	CI	Composition	E(ev)	Oscillator strength (<i>f</i>)	λ_{theo}
$S_0 \rightarrow S_1$	0.66889	H → L (89%)	1.9297	0.1785	642.50
$S_0 \rightarrow S_4$	0.54911	H-1 → L+1 (60%)	2.1674	0.0909	572.04
	0.29142	H-1 → L+2 (17%)			
$S_0 \rightarrow S_{11}$	0.64828	H-3 → L (84%)	2.8765	0.0401	431.04
$S_0 \rightarrow S_{14}$	0.60535	H-3 → L+1 (73%)	3.0657	0.2304	404.42
$S_0 \rightarrow S_{17}$	0.45057	H-2 → L+3 (41%)	3.2041	0.1265	386.95
	-0.28328	H-3 → L+2 (16%)			
	-0.04599	H-3 → L+1 (15%)			
$S_0 \rightarrow S_{26}$	0.54771	H-2 → L+3 (60%)	3.4825	0.0364	356.02
	-0.21939	H-3 → L+1 (10%)			
$S_0 \rightarrow S_{55}$	0.31831	H-5 → L+2 (20%)	3.9374	0.0168	314.88
	0.27083	H-4 → L+3 (15%)			
	0.26714	H-1 → L+10 (14%)			

λ_{expt}		Hole	Electron
694 nm	S_1 $w = 0.89$ 1.9297 (0.1785) 642.50 nm		
	$^1\text{ILCT}/^1\text{LMCT}$ $\pi(\text{N}_{\text{amido-nb}} + \text{Ph}) \rightarrow \pi^*(\text{azo} + \text{Ph}) + 4d_z^2(\text{Rh})$		
654 nm	S_4 $w = 0.60$ 2.1674 (0.0909) 572.04 nm		
	$^1\text{ILCT}/^1\text{LMCT}$ $\pi(\text{N}_{\text{amido-nb}} + \text{Ph}) \rightarrow \pi^*(\text{azo} + \text{Ph}) + 4d_z^2(\text{Rh})$		
371 nm	S_{17} $w = 0.41$ 3.2041 (0.1265) 386.95 nm		
	$^1\text{LMCT}/^1\text{ILCT}$ $\pi(\text{N}_{\text{amido-nb}} + \text{Ph}) \rightarrow 4d_x^2 - y^2(\text{Rh}) + \pi^*(\text{N}_{\text{amido-b}})$		
313 nm	S_{26} $w = 0.60$ 3.4825 (0.0364) 356.002		
	$^1\text{LMCT}/^1\text{ILCT}$ $\pi(\text{Ph}) \rightarrow 4d_z^2(\text{Rh}) + \pi^*(\text{azo})$		

Fig. S12 Natural transition orbitals (NTOs) for complex **3** illustrating the nature of singlet excited states in the absorption bands in the range 300–700 nm. For each state, the respective number of the state, transition energy (eV), and the oscillator strength (in parentheses) are listed. Shown are only occupied (holes) and unoccupied (electrons) NTO pairs that contribute more than 40% to each excited state

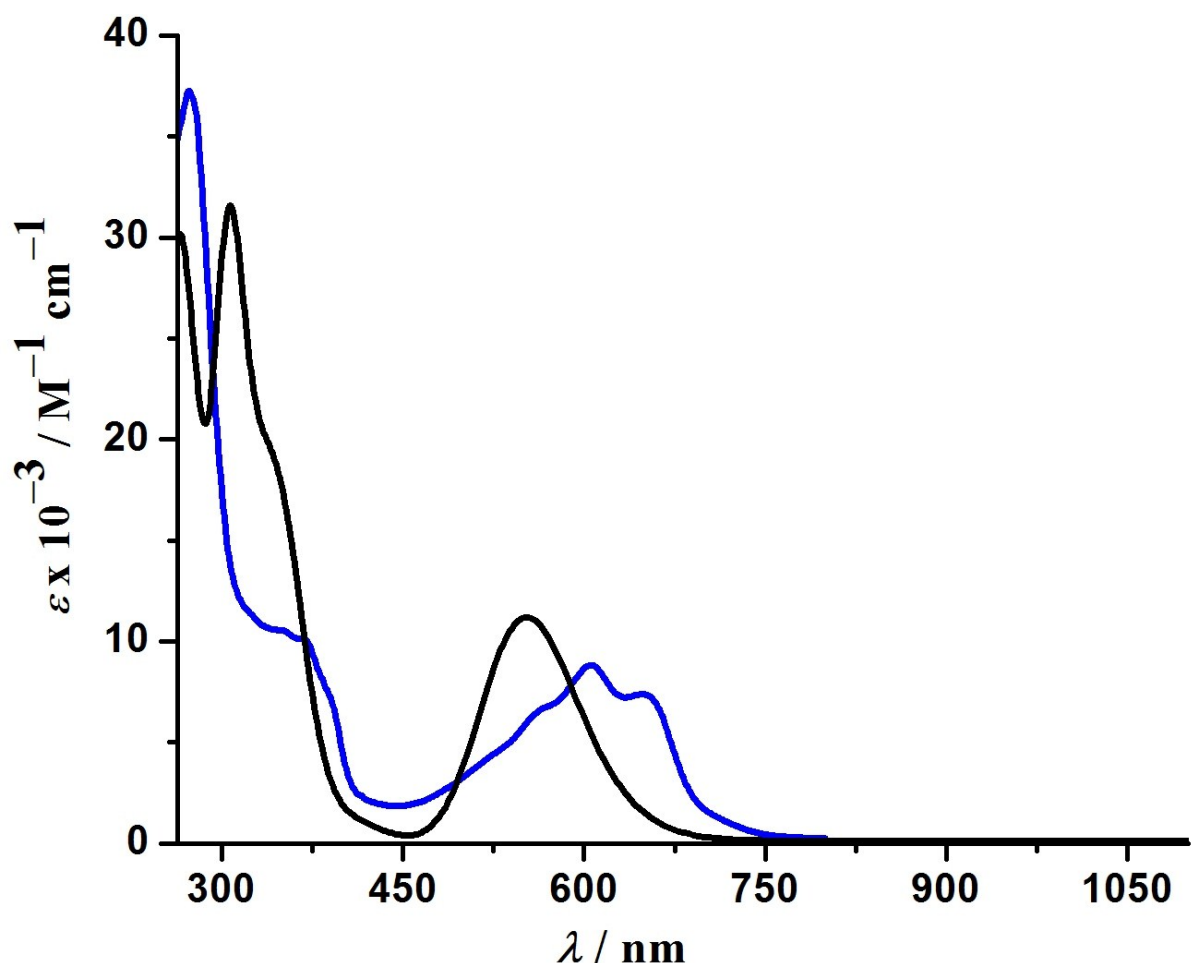


Fig. S13 Experimental (blue) and theoretical (black) absorption spectra of **2** in dichloromethane.

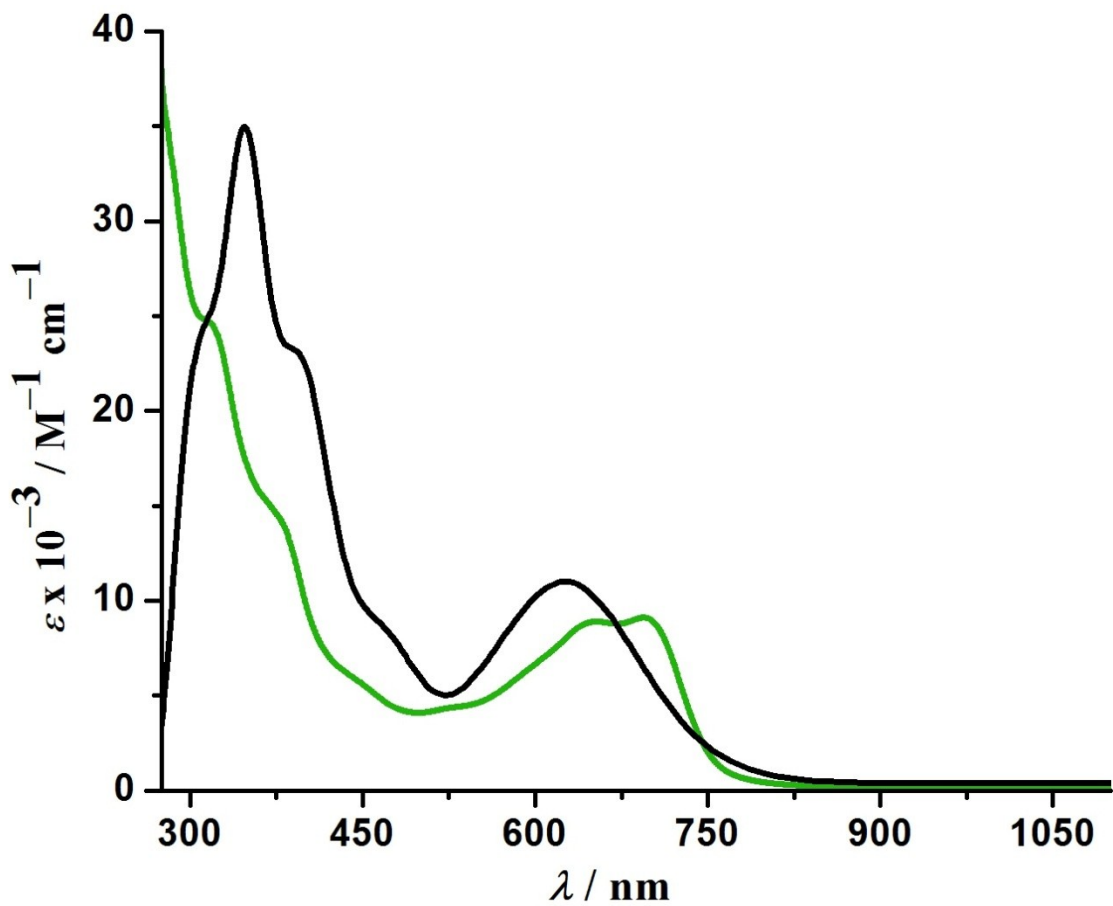


Fig. S14 Experimental (green) and theoretical (black) absorption spectra of **3** in dichloromethane.

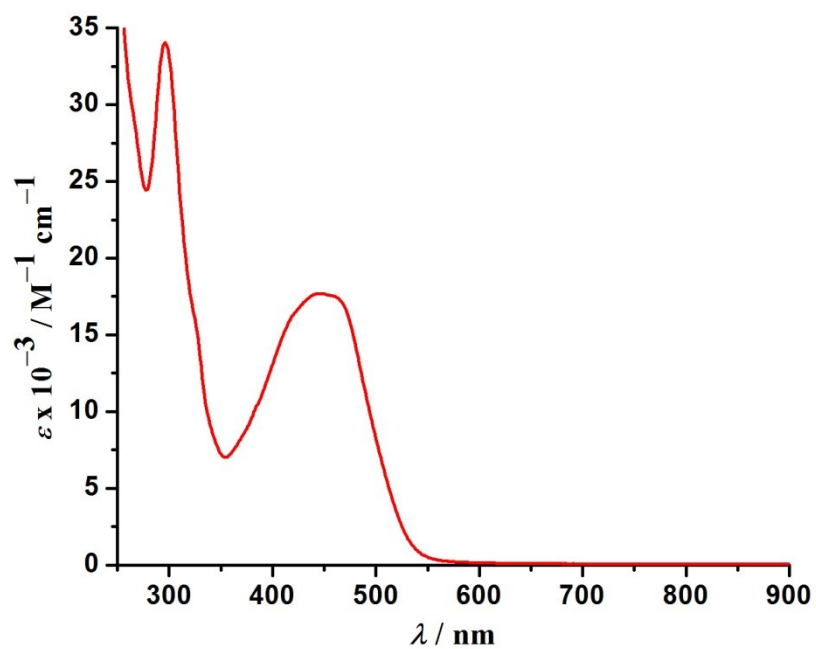


Fig. S15 Experimental absorption spectrum of ligand **1** in CH_2Cl_2 at room temperature.

Table S8 Coordinates of optimized geometry ¹²

Tag	Symbol	X	Y	Z
1	Rh	10.22673	9.763149	8.050288
2	P	9.352287	11.92466	7.385007
3	C1	9.934983	9.100642	5.723029
4	C1	11.14132	7.565504	8.582604
5	N	12.28542	10.28189	7.85831
6	H	12.68046	9.367177	7.612049
7	H	12.51593	10.94549	7.117365
8	N	10.57366	10.19773	9.98406
9	N	9.802943	10.04184	10.99214
10	N	8.395354	9.105769	8.502435
11	H	7.891247	8.643182	7.750348
12	C	7.874745	9.026536	9.713146
13	C	6.574752	8.435393	9.913837
14	H	6.070921	8.02264	9.042672
15	C	5.983935	8.381507	11.14911
16	H	5.001703	7.924882	11.24776
17	C	6.634304	8.903812	12.30588
18	H	6.150814	8.850191	13.27632
19	C	7.882507	9.451475	12.17176
20	H	8.424212	9.839022	13.02956
21	C	8.55301	9.531423	10.90764
22	C	11.89459	10.63686	10.25049
23	C	12.34981	11.0002	11.52952
24	H	11.66825	10.91925	12.36791
25	C	13.65482	11.45545	11.69848
26	H	13.99683	11.73743	12.6908
27	C	14.52671	11.54963	10.60597
28	H	15.54423	11.90422	10.74229
29	C	14.0836	11.17139	9.336901
30	H	14.75376	11.21883	8.481659
31	C	12.77735	10.71702	9.157904
32	C	8.862042	13.09495	8.731755
33	C	9.773535	13.35422	9.770069
34	H	10.74145	12.86631	9.783027

35	C	9.457671	14.25078	10.79196
36	H	10.17816	14.4338	11.58483
37	C	8.221244	14.90311	10.79731
38	H	7.971386	15.59566	11.5969
39	C	7.311253	14.66134	9.766155
40	H	6.350163	15.16899	9.754128
41	C	7.629136	13.76848	8.737933
42	H	6.91218	13.60565	7.941289
43	C	10.57474	12.90561	6.395468
44	C	10.80373	14.26948	6.644309
45	H	10.25676	14.78276	7.427597
46	C	11.73575	14.98372	5.885045
47	H	11.89915	16.03801	6.093334
48	C	12.44918	14.3496	4.865215
49	H	13.17305	14.90673	4.275939
50	C	12.22155	12.99493	4.603952
51	H	12.76124	12.49333	3.804483
52	C	11.29313	12.27441	5.360905
53	H	11.10295	11.22723	5.136849
54	C	7.852117	11.80346	6.322643
55	C	7.853592	12.22604	4.985912
56	H	8.74966	12.64773	4.544454
57	C	6.703013	12.10137	4.202086
58	H	6.724465	12.42923	3.166073
59	C	5.537769	11.55394	4.741961
60	H	4.645095	11.45441	4.129947
61	C	5.526545	11.13335	6.075378
62	H	4.623932	10.70919	6.507919
63	C	6.674579	11.25386	6.860185
64	H	6.648756	10.92419	7.893195

Table S9 Coordinates of optimized geometry **¹3** (*syn* form)

Tag	Symbol	X	Y	Z
1	Rh	-1.58064	-0.49094	0.230586
2	Rh	1.550703	0.488804	0.307366
3	Cl	-1.41543	-1.21894	2.574708
4	Cl	1.27446	1.126387	2.675634
5	P	-3.70533	0.510086	0.856476
6	P	3.663033	-0.56946	0.847072
7	N	-2.43108	-2.30555	-0.06564
8	H	-2.56676	-2.88505	0.759195
9	N	-2.29953	-0.79849	-2.66082
10	N	-1.76741	-0.08499	-1.74652
11	N	-0.47994	1.318543	0.128318
12	H	-0.47374	1.959697	0.919739
13	N	2.429583	2.306608	0.121468
14	H	2.579855	2.838239	0.974663
15	N	2.294085	0.953414	-2.55686
16	N	1.778802	0.177709	-1.68372
17	N	0.452529	-1.31668	0.084501
18	H	0.400977	-1.99654	0.840599
19	C	-2.90949	-2.77693	-1.20867
20	C	-3.54037	-4.06995	-1.26996
21	H	-3.60462	-4.64242	-0.3466
22	C	-4.03413	-4.58773	-2.44325
23	H	-4.49575	-5.57292	-2.43569
24	C	-3.95117	-3.86031	-3.66209
25	H	-4.34665	-4.28083	-4.58157
26	C	-3.36395	-2.61846	-3.6502
27	H	-3.27889	-2.02651	-4.55692
28	C	-2.83206	-2.03402	-2.46054
29	C	-1.3277	1.210608	-2.12267
30	C	-1.51411	1.758649	-3.40011
31	H	-1.94754	1.141477	-4.17847
32	C	-1.18385	3.091269	-3.63041
33	H	-1.33793	3.52255	-4.616
34	C	-0.6769	3.882012	-2.58678

35	H	-0.43889	4.927927	-2.76176
36	C	-0.45479	3.326703	-1.3283
37	H	-0.0337	3.926476	-0.52674
38	C	-0.7467	1.973133	-1.08547
39	C	-4.84005	1.056396	-0.50415
40	C	-4.41437	2.091785	-1.35589
41	H	-3.45223	2.568013	-1.20125
42	C	-5.22588	2.536464	-2.40012
43	H	-4.87329	3.337871	-3.0438
44	C	-6.47771	1.953087	-2.61753
45	H	-7.10794	2.297062	-3.43375
46	C	-6.91392	0.929717	-1.77428
47	H	-7.88896	0.473378	-1.92533
48	C	-6.10427	0.486613	-0.72353
49	H	-6.475	-0.29545	-0.07161
50	C	-3.48055	2.050972	1.853775
51	C	-2.38285	2.160205	2.724729
52	H	-1.66582	1.350006	2.810129
53	C	-2.21747	3.306145	3.508605
54	H	-1.35697	3.373238	4.168791
55	C	-3.14404	4.34946	3.439641
56	H	-3.01156	5.240336	4.048783
57	C	-4.24496	4.242287	2.584166
58	H	-4.97497	5.045957	2.527049
59	C	-4.4144	3.101027	1.796678
60	H	-5.27523	3.034369	1.139371
61	C	-4.74754	-0.5746	1.929478
62	C	-5.06224	-0.20153	3.244791
63	H	-4.69757	0.735948	3.649136
64	C	-5.83817	-1.03569	4.054579
65	H	-6.06582	-0.7298	5.072476
66	C	-6.31084	-2.25442	3.564518
67	H	-6.91286	-2.9029	4.195975
68	C	-6.00116	-2.63627	2.255982
69	H	-6.36348	-3.58223	1.86095
70	C	-5.22131	-1.80749	1.446766
71	H	-4.9893	-2.12715	0.437061
72	C	2.924604	2.833738	-0.98862

73	C	3.585427	4.113533	-0.96941
74	H	3.686812	4.611428	-0.00737
75	C	4.069114	4.703363	-2.11046
76	H	4.555135	5.67416	-2.04123
77	C	3.948813	4.066604	-3.37797
78	H	4.334616	4.545753	-4.27263
79	C	3.343521	2.836228	-3.44304
80	H	3.23329	2.310761	-4.38747
81	C	2.823876	2.17602	-2.28603
82	C	1.375338	-1.1084	-2.1273
83	C	1.608627	-1.59782	-3.42042
84	H	2.06743	-0.94648	-4.15501
85	C	1.281932	-2.91608	-3.72444
86	H	1.472925	-3.30235	-4.72207
87	C	0.732413	-3.75094	-2.73919
88	H	0.494479	-4.78546	-2.97294
89	C	0.471271	-3.25598	-1.46376
90	H	0.018819	-3.89083	-0.70737
91	C	0.76232	-1.91804	-1.14738
92	C	4.397187	-1.50565	-0.56536
93	C	4.368438	-2.90812	-0.61631
94	H	3.935977	-3.47591	0.200619
95	C	4.897252	-3.59067	-1.71575
96	H	4.864769	-4.67692	-1.73624
97	C	5.458161	-2.88353	-2.78081
98	H	5.871323	-3.41573	-3.63388
99	C	5.473478	-1.48577	-2.74939
100	H	5.894709	-0.9227	-3.57837
101	C	4.940395	-0.80267	-1.65577
102	H	4.953569	0.283123	-1.65567
103	C	5.03159	0.54699	1.419419
104	C	4.749537	1.472496	2.440369
105	H	3.74199	1.546336	2.838924
106	C	5.760683	2.284252	2.958246
107	H	5.523771	2.990029	3.750688
108	C	7.066728	2.189704	2.468095
109	H	7.851532	2.824782	2.871486
110	C	7.356679	1.267287	1.461225

111	H	8.369401	1.175997	1.076236
112	C	6.348536	0.447931	0.942489
113	H	6.603694	-0.26794	0.169193
114	C	3.586827	-1.80679	2.218576
115	C	4.767122	-2.46003	2.620605
116	H	5.709849	-2.23811	2.128062
117	C	4.742091	-3.39523	3.654891
118	H	5.662116	-3.8914	3.953909
119	C	3.538167	-3.68623	4.307789
120	H	3.519384	-4.41234	5.116846
121	C	2.367711	-3.03011	3.925297
122	H	1.429455	-3.23032	4.435544
123	C	2.388911	-2.09016	2.888228
124	H	1.478518	-1.55497	2.647815

Table S10 Coordinates of optimized geometry ¹³ (*anti* form)

Tag	Symbol	X	Y	Z
1	Rh	-3.88627	0.328557	12.60372
2	C1	-2.36569	0.115448	10.69138
3	P	-2.06987	-0.74083	13.85367
4	N	-5.08469	0.354287	14.2246
5	N	-5.30214	1.293668	15.05389
6	C	-3.63211	2.93207	14.07261
7	C	-3.10845	4.258686	14.27171
8	H	-2.30057	4.581278	13.61813
9	C	-3.60072	5.106215	15.2345
10	H	-3.17368	6.101916	15.33272
11	C	-4.65094	4.702845	16.10349
12	H	-5.03039	5.381187	16.86148
13	C	-5.16404	3.434761	15.97144
14	H	-5.95663	3.075978	16.6222
15	C	-4.69697	2.517771	14.98104
16	C	-5.67897	-0.9116	14.47961
17	C	-6.25519	-1.27511	15.69999
18	H	-6.29621	-0.54743	16.5019
19	C	-6.74326	-2.56856	15.86803
20	H	-7.17636	-2.86119	16.82071
21	C	-6.65854	-3.49568	14.81964
22	H	-7.02651	-4.50923	14.95917
23	C	-6.10794	-3.12537	13.59215
24	H	-6.06437	-3.83371	12.7685
25	C	-5.62071	-1.82478	13.40329
26	C	-1.34752	-2.29992	13.16558
27	C	-0.19662	-2.85295	13.75458
28	H	0.276844	-2.35789	14.59738
29	C	0.353008	-4.03761	13.26248
30	H	1.244552	-4.45043	13.72787
31	C	-0.23747	-4.68531	12.17191
32	H	0.193376	-5.60556	11.78542
33	C	-1.37371	-4.13674	11.57473
34	H	-1.82905	-4.62034	10.71448

35	C	-1.92291	-2.94849	12.06637
36	H	-2.77049	-2.50248	11.56464
37	C	-0.55587	0.312784	14.10206
38	C	0.101701	0.400711	15.34079
39	H	-0.28762	-0.11526	16.21094
40	C	1.273139	1.152987	15.47582
41	H	1.762203	1.208471	16.44532
42	C	1.811628	1.822637	14.37575
43	H	2.722278	2.40705	14.48146
44	C	1.171956	1.729225	13.13631
45	H	1.585136	2.236341	12.26778
46	C	-0.00036	0.983157	12.99765
47	H	-0.47902	0.905355	12.02696
48	C	-2.54078	-1.21648	15.57754
49	C	-2.68444	-2.55811	15.96356
50	H	-2.50514	-3.35476	15.24964
51	C	-3.05904	-2.88572	17.26997
52	H	-3.16607	-3.93087	17.54864
53	C	-3.29663	-1.87979	18.20833
54	H	-3.58373	-2.13611	19.22504
55	C	-3.17315	-0.53936	17.82926
56	H	-3.36564	0.254194	18.54681
57	C	-2.80588	-0.21051	16.52405
58	H	-2.71726	0.836572	16.25063
59	Rh	-6.70919	-0.31531	11.00088
60	Cl	-8.22963	-0.10241	12.91337
61	P	-8.5256	0.754237	9.751038
62	N	-5.5108	-0.34109	9.379978
63	N	-5.29342	-1.28048	8.550679
64	C	-6.96351	-2.9188	9.531978
65	C	-7.48725	-4.24539	9.332879
66	H	-8.29513	-4.56794	9.986471
67	C	-6.99505	-5.09293	8.370063
68	H	-7.42215	-6.08861	8.27184
69	C	-5.94484	-4.68961	7.501049
70	H	-5.56544	-5.36796	6.743033
71	C	-5.43166	-3.42155	7.633099
72	H	-4.63907	-3.0628	6.982322

73	C	-5.89865	-2.50455	8.623521
74	C	-4.91645	0.924761	9.124956
75	C	-4.34018	1.288221	7.90458
76	H	-4.29917	0.560514	7.102693
77	C	-3.85205	2.581647	7.736522
78	H	-3.41891	2.87423	6.78385
79	C	-3.93677	3.508797	8.784892
80	H	-3.56875	4.522326	8.64535
81	C	-4.48741	3.138541	10.01238
82	H	-4.53098	3.846895	10.83601
83	C	-4.97469	1.837971	10.20126
84	C	-9.24784	2.313406	10.4391
85	C	-10.3987	2.866477	9.850011
86	H	-10.8721	2.371418	9.007195
87	C	-10.9483	4.05117	10.34206
88	H	-11.8398	4.464006	9.876607
89	C	-10.3578	4.698873	11.43264
90	H	-10.7887	5.61915	11.81908
91	C	-9.22164	4.150291	12.02987
92	H	-8.76631	4.633902	12.89012
93	C	-8.67245	2.962003	11.53829
94	H	-7.8249	2.515989	12.04008
95	C	-10.0397	-0.29926	9.502478
96	C	-10.6973	-0.38681	8.263762
97	H	-10.308	0.129429	7.393748
98	C	-11.8688	-1.13902	8.128557
99	H	-12.3579	-1.19418	7.159069
100	C	-12.4072	-1.80902	9.228442
101	H	-13.3178	-2.3934	9.122605
102	C	-11.7674	-1.71603	10.46787
103	H	-12.1805	-2.22345	11.33626
104	C	-10.5951	-0.97	10.60671
105	H	-10.1163	-0.89257	11.57738
106	C	-8.05466	1.229883	8.027185
107	C	-7.9109	2.571512	7.641179
108	H	-8.09012	3.368163	8.355118
109	C	-7.5363	2.899097	6.334766
110	H	-7.42919	3.94424	6.056105

111	C	-7.29881	1.893161	5.396387
112	H	-7.0117	2.149469	4.379684
113	C	-7.42241	0.552738	5.775448
114	H	-7.22998	-0.24083	5.057878
115	C	-7.78968	0.223901	7.080661
116	H	-7.87838	-0.82318	7.354068
117	N	-5.47779	1.346843	11.42072
118	N	-5.11764	-1.3336	12.18383
119	N	-7.44196	-2.13741	10.49459
120	N	-3.15359	2.15069	13.11002
121	H	-2.39159	2.539901	12.56232
122	H	-8.20397	-2.52657	11.04231
123	H	-4.80853	-2.08991	11.57774
124	H	-5.78689	2.103196	12.02676